International Journal of Applied Earth Observation and Geoinformation 146 (2026) 105157

Contents lists available at ScienceDirect

International Journal of Applied Earth Observation and Geoinformation

journal homepage: www.elsevier.com/locate/jag

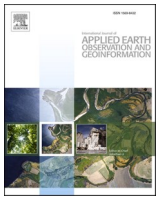

Forest canopy cover loss dynamics in Germany between 2017 and 2024: Revealing regional differences

Frank Thonfeld [a,*], Patrick Kacic [b], Stefanie Holzwarth [a], Marco Wegler [a], Sarah Asam [a], Claudia Kuenzer [a,b]

[a] German Aerospace Center (DLR), German Remote Sensing Data Center (DFD), 82234 Oberpfaffenhofen, Wessling, Germany
[b] University of Würzburg, Institute of Geography and Geology, Department of Remote Sensing, Am Hubland, 97074 Würzburg, Germany

ARTICLE INFO

Keywords:
Time series
Remote sensing
Disturbance
Drought
Harvest
Sentinel
Landsat

ABSTRACT

From 2018 onwards, multiple droughts and heatwaves hit Central Europe including Germany. These triggered, together with other disturbance drivers, unprecedented damages to forests. While annual field-based crown defoliation surveys provide valuable insights into overall forest condition in Germany, continuous spatio-temporal dynamics are not explicitly addressed in current monitoring practices. Here, we present a forest canopy cover loss (FCCL) assessment in Germany at monthly resolution between September 2017 and September 2024 based on Sentinel-2 and Landsat satellite time series. This approach enables near-continuous monitoring of forest disturbance dynamics across spatial and temporal scales. Our results reveal that a strip in central Germany was most affected. Storm events in late 2017 and early 2018 caused the first large-scale canopy losses, while drought- and heat-related disturbances, including bark beetle outbreaks in spruce forests, dominated in 2019 and 2020. FCCL rates generally declined after 2020. We recorded a total of 924,000 ha FCCL over the seven-year period (8.4% of Germany's forest area), 84.5% of which were found in coniferous forests. At district and municipality level, we detected FCCL of up to more than 50%. Two-thirds of FCCL were recorded during winter (November-April), underscoring the importance of off-season monitoring. This study demonstrates the value of dense, multi-sensor satellite time series for operational forest monitoring. It highlights regions with high future disturbance potential, particularly in southern and southeastern Germany due to their high share of spruce forests. Future monitoring should integrate seasonal data and early-warning systems to improve adaptive forest management at national scale.

1. Introduction

Between 2018 and 2020, Central Europe, including Germany, was hit by the most severe drought in terms of soil moisture deficit in the past 250 years, with respect to extent, duration, and intensity (Rakovec et al., 2022). This drought forms the background against which forest condition in Germany worsened dramatically (BMLEH, 2025). Crown condition is typically assessed annually in the field using fixed plots, with crown defoliation as a key indicator. These assessments reveal a long-term deteriorating trend since the assessments started in 1984, reflecting increasing impacts of natural disturbances in Europe (Patacca et al., 2023). In recent years, however, forests with $\geq$ 30% crown defoliation increased sharply in Germany, while the share of forests without crown defoliation dropped to 20%, despite above-average precipitation in 2023 and 2024 (2025). Forests were impacted not only by large storms but also by droughts, heatwaves, cascading insect infestations, and forest management interventions such as sanitary and salvage logging. It is often difficult or even impossible to disentangle these multiple hazards (de Brito, 2021). These disturbances led to extensive early wilting and stress symptoms (Brun et al., 2020; Descals et al., 2023), but also to exceptionally high rates of forest decline in Germany and other Central European countries (Arthur et al., 2024; Buras et al., 2021; T. Hlásny et al., 2021; Schuldt et al., 2020; Senf and Seidl, 2021; Thonfeld et al., 2022).

According to the latest national forest inventory (2021/2022), only four dominant tree species – pine, spruce, beech, and oak – cover about 72% of Germany's forest area. Pine is now slightly more abundant than spruce (21.8% vs. 20.9%). Spruce suffered from doughts and bark beetle

* Corresponding author.
E-mail addresses: frank.thonfeld@dlr.de (F. Thonfeld), patrick.kacic@dlr.de (P. Kacic), stefanie.holzwarth@dlr.de (S. Holzwarth), marco.wegler@dlr.de (M. Wegler), sarah.asam@dlr.de (S. Asam), claudia.kuenzer@dlr.de (C. Kuenzer).

https://doi.org/10.1016/j.jag.2026.105157
Received 6 August 2025; Received in revised form 22 January 2026; Accepted 3 February 2026

infestations, losing about 16.8% of its area compared to the previous inventory in 2012 (2024). Yet, spruce has an outstanding value in the timber industry.

Earth Observation (EO) has long played a key role in the analysis of forests from local to regional scales (Holzwarth et al., 2020). The increased data availabilty from the Sentinel-2 satellites compared to the previously dominant source of Landsat data and the recent "forest dieback 2.0" (Mack et al., 2023) set the ground for a shift towards large-scale monitoring of disturbances (Holzwarth et al., 2023).

The first EO-based nation-wide forest product was the tree canopy cover loss data set (Thonfeld et al., 2022), providing 10 m resolution information at monthly intervals but only covering 2018–2021. Recent complementary EO products map dominant tree species (Blickensdörfer et al., 2024; Wegler et al., 2025; Welle et al., 2022) and forest condition (Buras et al., 2021; Gnilke and Sanders, 2022; Lange et al., 2024). supporting applications like mortality modelling (Knapp et al., 2024), canopy cover loss prediction due to bark beetle infestations (Shrestha et al., 2025) or species-specific drought response (Wang et al., 2025; Xu et al., 2025). Advanced methods, including convolutional neural network (CNN) and transformers applied to Sentinel-1/2 or UAV data, allow detection of standing dead trees and mapping of forest disturbances (Schiefer et al., 2023; Schiller et al., 2024).

Large-scale forest disturbance products at global to continental scale have predominantly relied on Landsat data due to its long-term record (Hansen et al., 2013; Turubanova et al., 2023; Viana-Soto and Senf, 2025). These datasets typically map disturbances at annual intervals with 30 m resolution. While useful for long-term trends, they do not capture subannual, seasonal dynamics, which are critical for understanding the timing and drivers of forest loss. Despite the spectral similarity between Landsat and Sentinel-2, there is currently no countrywide study in Germany that combines both datasets to exploit the higher temporal resolution and denser coverage of Sentinel-2 (Li and Roy, 2017). Consequently, information on the seasonal progression of forest disturbances at regional to national scales remains limited. Here, we address this gap by revising and extending the work by Thonfeld et al. (2022) to quantify forest canopy cover loss (FCCL) dynamics across Germany from September 2017 to September 2024, hence encompassing both the 2017/2018 winter storm season and the recent drought and heat years.

Our objectives are to;

(i) introduce methodological improvements to combine Sentinel-2 and Landsat data for FCCL monitoring,
(ii) provide an updated and detailed assessment of recent FCCL patterns, including the emergence and disappearance of hotspots, and
(iii) identify forest areas at high risk of future FCCL and the environmental and ecological factors that increase regional susceptibility.

2. Methods

2.1. Data and pre-processing

Building upon the approach presented in Thonfeld et al. (2022), we used all available level 2 surface reflectance data from Sentinel-2 A/B and Landsat-8/9 over Germany acquired between January 1, 2017 and September 30, 2024 with less than 80% cloud cover (Appendix C), a common threshold for using dense time series of optical satellite data in temperate forests (Zhu and Woodcock, 2014). We applied sensor-specific cloud, cloud shadow, and snow masks to the data collections of the two different sensor systems to ensure clear pixels. Afterwards we used the spectrally similar bands in the visible, near-infrared, and short-wave infrared domains and merged the data to a common collection. For each individual image we applied a tasseled cap transformation and used the components brightness, greenness, and wetness to compute the disturbance index (DI, Healey et al., 2005). This includes normalization of the tasseled cap components using their mean and standard deviation of forest pixels. The normalization step therefore involves a forest mask. We used the stocked forest map of the year 2018 (Langner et al., 2022). In addition, this stocked forest map was overlaid with a reclassified tree species map (Blickensdörfer et al., 2024) to differentiate between forest types. Pixels of the classes birch, beech, oak, alder, deciduous trees with long lifespan and deciduous trees with short lifespan were classified as deciduous forest and pixels of the classes Douglas fir, spruce, pine, larch and fir as coniferous forest. The coverage of the two datasets is not identical, which is why a few areas of the forest reference map remained unclassified. These were filled with the dominant leaf type map 2015 of the Copernicus Land Monitoring Service (CLMS 2025). Forest areas that could not be labelled with a forest type remained unclassified. Based on the resulting forest type map we applied the normalization step of deciduous and coniferous forest pixels individually. After normalization, we filtered the DI time series with a running median filter with thirty-day length to remove outliers due to undetected clouds, cloud shadows or snow.

2.2. Forest canopy cover loss detection

The DI is less insensitive to seasonal variation and phenology than other spectral indices. We used the pixel-wise median of 2017 DI images as a reference, which allows us to cover the 2017/2018 winter storm season in the monitoring period and benefits from increased data availability after Sentinel-2B became operational (Appendix C). For the whole observation period (September 2017 to September 2024), we generated monthly DI composites using the 10th percentile. We then computed the difference between each composite of the observation period and the 2017 reference composite. DI values of healthy forests are usually slightly negative while disturbed pixels have considerably high positive values. We therefore applied an empirically determined threshold of 2, that was reliable in Thonfeld et al. (2022). Application of the threshold to each difference image results in an individual binary time series for each pixel with 0 indicating normal conditions and 1 indicating threshold exceedance. As the goal of the approach is the detection of forest canopy cover losses, we assume a certain duration of the anomaly rather than short-term anomalies. We therefore record a pixel as FCCL if the threshold was exceeded at least six consecutive times, corresponding to a minimum period of six months. However, we removed pixels that showed anomalies only in winter, which happens sometimes in deciduous forests. In its initial form (Thonfeld et al., 2022) the method considered only anomalies as FCCL that lasted until the end of the time series. With this modification we are now able to account for forest areas that experience re-greening after canopy cover losses during the observation period.

From the binary time series, we were able to retrieve several auxiliary layers. First, we classified the time series into intact forest, consistent FCCL, and temporal anomalies in deciduous, coniferous, and unclassified forests based on a rule-based decision tree and the intersection with the forest type map. The decision tree is a deterministic, rule-based classification scheme that applies a set of predefined logical criteria to the binary FCCL time series and does not involve machine learning. FCCL pixels are classified as temporal anomalies if the anomaly lasts less than two growing seasons and is followed by a period of normal conditions (i.e. DI threshold not exceeded). Toward the end of the observation period, such a distinction is not possible due to missing follow-up observations. Temporal anomalies can occur when forests recover from insect infestations or drought response. However, bark beetle infestations in spruce are usually fatal. Second, we computed how often the threshold was exceeded per pixel. This allows a qualitative inspection if pixels are prone to exceptional dynamics or if anomalies are consistent. Third, we computed the percentage of gaps (i.e., observations where the threshold was not exceeded) in pixels labelled as FCCL.

2.3. Validation

We used the validation dataset generated by Reinosch et al. (2024) based on a comprehensive reference dataset (Langner et al., 2024). This validation dataset contains 11,019 points, distributed over the major forest regions in Germany and each enriched with information about disturbance type (or absence of disturbance), severity, date, and auxiliary information covering the period from 2018 to 2022. We limited our map to the same time frame, converted the time information of FCCL to a binary disturbed/undisturbed map, and stratified the map into disturbed, undisturbed and a buffer class following the procedure of Reinosch et al. (2024). The buffer extends 10 m (i.e. one pixel) inside and outside the disturbed areas. We removed points with inconsistent or incomplete information. Samples labelled as undisturbed in the validation data that show FCCL later than 2022 were also removed as it is unclear whether these are commission errors or represent a later event not present in the reference. According to the best practices proposed by Olofsson et al. (2014), sample sizes should be derived from the proportions of each stratum. Since we wanted to modify the fully independent validation data as little as possible, we didn't adjust the sample size, but rather used the data from Reinosch et al. (2024) and the sample sizes that fit to their results and located them in our strata. This resulted in 1578 points for disturbed, 5810 points for undisturbed, and 1286 points for the buffer stratum, hence 8674 in total. We computed standard accuracy metrics (overall accuracy (OA), user's (UA) and producer's accuracy (PA), F1-score) for each stratum and also for the entire dataset without stratification.

2.4. Aggregation to larger spatial units

To provide information for administrations and policymakers, we aggregated the pixel-based results to administrative levels (municipality, district, federal state). Administrative data (BKG, 2025) is updated at annual intervals to account for new legislations. It contains 10,957 entities at municipality level, 400 at district level and 16 at federal state level. Aggregations distinguish deciduous, coniferous, unclassified, and total forest areas. We computed percentages in relation to the forest area per polygon and per forest type based on the forest type map (Section 2.1). July–September 2024 were excluded from annual statistics due to incomplete anomaly criteria and are provided as a low-confidence attribute. To assess continuous spatial patterns and relate our results to tree species distribution, we also aggregated the pixel-based results to hexagons. These have an equal area and are therefore suitable for regional comparisons.

2.5. FCCL and environmental factors

To better understand the relationship between FCCL and the site characteristics, we aggregated the pixel-based results to forest growth districts and forest growth regions (Gauer and Kroiher, 2012). Forest growth districts reflect rather homogeneous environmental conditions with respect to landscape, climate, geology, topography, vegetation composition, and forest history and development. They are distinct from neighbouring forest growth districts. Forest growth districts are aggregated to larger units to form forest growth regions. The maps are in scale 1:25,000 and consist of 82 forest growth regions and 608 forest growth districts. The original dataset was published by Gauer and Aldinger (2005). The maps were updated in 2011 (Gauer and Kroiher, 2012). A total of 51 attributes are included to characterize each forest growth district (Appendix A), of which 43 were used as they contain the environmental variables. The variable m_ueber-nn refers to the altitude zone and indicates an elevation range. We converted this information in maximum elevation (elev_max), minimum elevation (elev_min), and the difference of the two (elev_diff) and deleted m_ueber_nn. We then applied a random forest regression model with 500 trees (Breiman, 2001; Liaw and Wiener, 2002) to quantify the statistical relationship between FCCL percentages and environmental variables of the forest growth districts. In contrast to the rule-based decision tree used for ancillary FCCL classification (Section 2.2), the random forest was employed solely as a machine-learning regression approach to assess variable importance and does not influence the FCCL detection itself. Random forest regression is an ensemble learning method that builds multiple regression trees using bootstrap samples of the data and random subsets of predictor variables at each split, thereby reducing variance and overfitting (Breiman, 2001). We computed the variable importance, expressed both as percent increase in mean squared error (%IncMSE) and Increase in Node Purity (IncNodePurity). The %IncMSE indicates how much worse a model performs (i.e., MSE increases) when a variable is randomly permuted. A higher %IncMSE means the variable is more important. The IncNodePurity shows how much a variable contributes to making pure splits in the random forest regression process (i.e., splits that separate the target variable well). A higher value means the variable helped make more effective splits.

2.6. Tree species-specific analysis

FCCL detection allowed us to identify hotspots and their development over time. Using the Thünen Institute's dominant tree species map (Blickensdörfer et al., 2024), we assessed which species are most affected by recent disturbances. This map achieved F1-scores between 0.72 and 0.97 in pure stands of the five dominant species, with an overall accuracy of 0.87. The accuracy per class decreased by 0.04–0.14 when plots of mixed stands were included. By overlaying FCCL results with species distribution and aggregating per hexagon, we produced a bivariate map showing the share of each dominant species alongside its corresponding FCCL, guiding targeted monitoring and forest management under recurrent drought and heat conditions.

3. Results

3.1. FCCL mapping accuracy

The validation of the FCCL product with independent reference data revealed very good results in the undisturbed (OA = 0.957) and the disturbed stratum (OA = 0.968) and moderate results in the buffer stratum (OA = 0.692, Table 1). Since the strata were derived from our map, there are only samples classified as disturbed in the disturbed stratum and samples classified as undisturbed in the undisturbed stratum. Hence, user's accuracy and producer's accuracy can exclusively be computed for the class contained in the respective stratum. Only the buffer stratum contains validation samples of both classes, disturbed and undisturbed. The overall metrics computed without stratification reveal very good results (overall accuracy 0.92 and F1 score of 0.90) with high UA's in both classes (Table 2). However, the PA and F1 score are lower for the disturbed class (0.80 and 0.86) compared to the undisturbed class (0.97 and 0.94, respectively).

3.2. FCCL in Germany for 2017–2024

Following the workflow outlined in Section 2, FCCL was mapped in Germany at monthly intervals from September 2017 to September 2024. The corresponding loss area amounts to 924,071 ha, exceeding the total forest area of both the states of Hesse and North Rhine-Westphalia. At national level, the FCCL reached 16,595 ha between September and December 2017 and increased sharply during 2018–2020, from 106,461 ha to 176,912 ha. Losses declined thereafter, reaching 87,415 ha in 2023. Between January and June 2024, an additional 67,591 ha of FCCL were recorded, followed by 87,253 ha of FCCL from July to September 2024. Fig. 1 illustrates the spatial distribution of FCCL across Germany between September 2017 and September 2024. The marginal plots reveal a pronounced concentration of FCCL along a west-east corridor in Central Germany. Northern Germany and southern

Table 1
Accuracy metrics for the stratified validation with 95% confidence intervals. N = number of samples, OA = Overall Accuracy, UA = User's Accuracy, PA = Producer's Accuracy.

Stratum	N	OA	UA undisturbed	PA undisturbed	UA disturbed	PA disturbed
Disturbed	1578	0.968 ± 0.0089	–	–	0.968 ± 0.0086	1.000 ± 0.0000
Buffer	1286	0.692 ± 0.0265	0.550 ± 0.0390	0.733 ± 0.0408	0.820 ± 0.0291	0.669 ± 0.0309
Undisturbed	5810	0.957 ± 0.0050	0.957 ± 0.0049	1.000 ± 0.0000	–	–

Table 2
Accuracy metrics of all validation points without stratification with 95% confidence intervals. OA = Overall Accuracy, UA = User's Accuracy, PA = Producer's Accuracy, F1 = F1 score.

Category	Metric	Value
Overall	OA	0.920 ± 0.0056
	F1 (macro)	0.901 ± 0.0070
Undisturbed	UA	0.919 ± 0.0067
	PA	0.972 ± 0.0043
	F1	0.944 ± 0.0041
Disturbed	UA	0.924 ± 0.0111
	PA	0.799 ± 0.0158
	F1	0.857 ± 0.0104

Germany, which has the highest share of forest, were less affected by FCCL.

Fig. 2 shows cumulative FCCL of all forest areas by federal state, expressed as percentage (left) and area in hectares (right).

In relative terms, North Rhine-Westphalia, Thuringia, Saxony-Anhalt, Saxony, Hesse, and Lower Saxony were most affected. Between 2017 and 2024, North Rhine-Westphalia lost about 17.1% of its forest canopy cover, followed by Thuringia (14.6%) and Saxony-Anhalt (10.0%.) All other federal states show losses below 10%.

In absolute terms, North Rhine-Westphalia and Bavaria each lost over 100,000 ha of forest, an area larger than metropolitan Berlin (89,000 ha). Ten of thirteen area-states lost more than 50,000 ha, with exceptions being the northern states Schleswig Holstein and Mecklenburg-Western Pomerania, the small state of Saarland, and the city-states Berlin, Hamburg, and Bremen.

Fig. 2 also reveals different temporal dynamics among federal states. Loss trajectories vary depending on local drought onset and local weather phenomena. North Rhine-Westphalia and Saxony-Anhalt show early, pronounced FCCL peaks followed by stabilization, whereas Thurinigia, Saarland and Bavaria exhibit relatively high FCCL percentages in recent years, indicating continuing canopy cover decline.

3.3. FCCL hotspot dynamics

Fig. 3 shows that first FCCL were recorded in 2017 in eastern Germany, particularly in the district of Passau (Bavaria), which was affected by the severe storm "Kolle" in late summer 2017. In 2018, FCCL spread over vast areas of Germany, with the highest values in north-eastern Germany and the Passau region, mainly due to winter storms such as "Friederike". The impacts of the 2018–2020 drought and heatwaves became visible in 2019 and 2020, with FCCL concentrated in the Harz region (central Germany) and in western Germany, gradually shifting from east to west. In 2021–2022, three hotspots of FCCL developed: the Harz region, low mountain ranges in western Germany, and the low mountain ranges along the border of Thuringia and Bavaria. In 2023–2024, FCCL was primarily concentrated in the latter region.

At the district level, Sonneberg (Thuringia), one of the most densely forested districts (~62% forest cover), had the highest total FCCL of 44.8%, followed by Oberbergischer Kreis (36.4%), Harz (36.0%), Kronach (35.2%), and Siegen-Wittgenstein (34.2%). In coniferous forests only, Sonneberg recorded a corresponding FCCL of 50.0%. The highest losses in coniferous forests occurred in Soest (62.8%), Oberbergischer Kreis (61.6%), Harz (60.9%), Göttingen (55.0%), and Märkischer Kreis (53.2%). Deciduous forest losses were lower, with the highest in Cottbus (7.4%), Meißen (7.0%), Hof (6.3%), Sonneberg (6.2%), and Groß-Gerau (5.7%). Overall, 65 of 400 districts experienced more than 10% FCCL of total forest, and 157 districts exceeded 10% FCCL in coniferous forests.

At municipality level, some areas lost about two-thirds of their forests. Forty-two municipalities exceeded 50% FCCL of total forest area, mostly in the Harz region and in the Thuringia-Bavaria border region. Regarding coniferous forests, 460 of 10,957 municipalities have more than 50% FCCL, and 4397 municipalities exceed 10% FCCL.

Fig. 4 presents cumulative FCCL for coniferous forests in percent (panel a) and in hectares (panel b) for seven selected districts from September 2017 to September 2024. FCCL occurred in all districts, but with different magnitudes and timing. The graphs highlight that considering both absolute area (ha) and percentage of forest cover is important, as districts vary in size and forest coverage. Hectare-wise, Sonneberg lost over 12,600 ha, while the Vogtlandkreis, Passau, and Soest lost 3,400–7,900 ha. Bonn experienced only 264 ha of FCCL. However, when expressed as a percentage of forest cover, losses are more pronounced: Soest lost over 60% of its coniferous forest, Sonneberg 50%, and even Bonn 26%. Vogtlandkreis lost more than 7% of coniferous forest cover.

The timing of FCCL acceleration varied between districts. Passau and Soest show early increases in 2017–2018, attributable to storm events and early drought. For other districts, extensive drought impacts became prominent between summer 2019 and mid-2021, causing accelerated loss due to massive tree mortality (browning), and bark beetle infestations, along with related sanitary logging. In Sonneberg, FCCL accelerated in mid-late 2019, and remained high, while Vogtlandkreis experienced moderate FCCL rates after 2018 storm events, but increasing again from 2023. Regular jumps in late winter/early spring indicate predominantly off-season forest management activities (Vogtlandkreis). FCCL in Passau, Bonn and Soest eventually plateaued; reaching stable levels by spring 2021–2022.

3.4. Environmental factors increasing regional susceptability to FCCL

With regard of forest growth types, the general patterns are similar to those observed at administrative unit level. However, because forest growth districts are relatively homogeneous and distinct from neighboring districts, differences are more pronounced and hotspots are clearly visible (Fig. 5). The twelve forest growth districts with the highest FCCL are concentrated in just five hotspot regions (Fig. 5), highlighting that central Germany's low mountain ranges experienced the most severe losses. Notably, there is no region without considerable FCCL. Regions with more than 10% FCCL occur throughout Germany, particularly in northeastern Germany and a strip in southern Germany.

The random forest regression relating environmental factors to total FCCL indicates that the share of spruce forest (fi_proz) per forest growth district is the most important predictor, both in terms of %IncMSE and IncNodePurity (Appendix B). Other important features with respect to %IncMSE include the 10% percentile of average January temperatures (tjan_min), the average of average January temperatures (tjan_mit), the 90% percentile of the climatic water balance per year (kwbj_max), the 90% percentile of the thermo-hygric index according to De Martonne

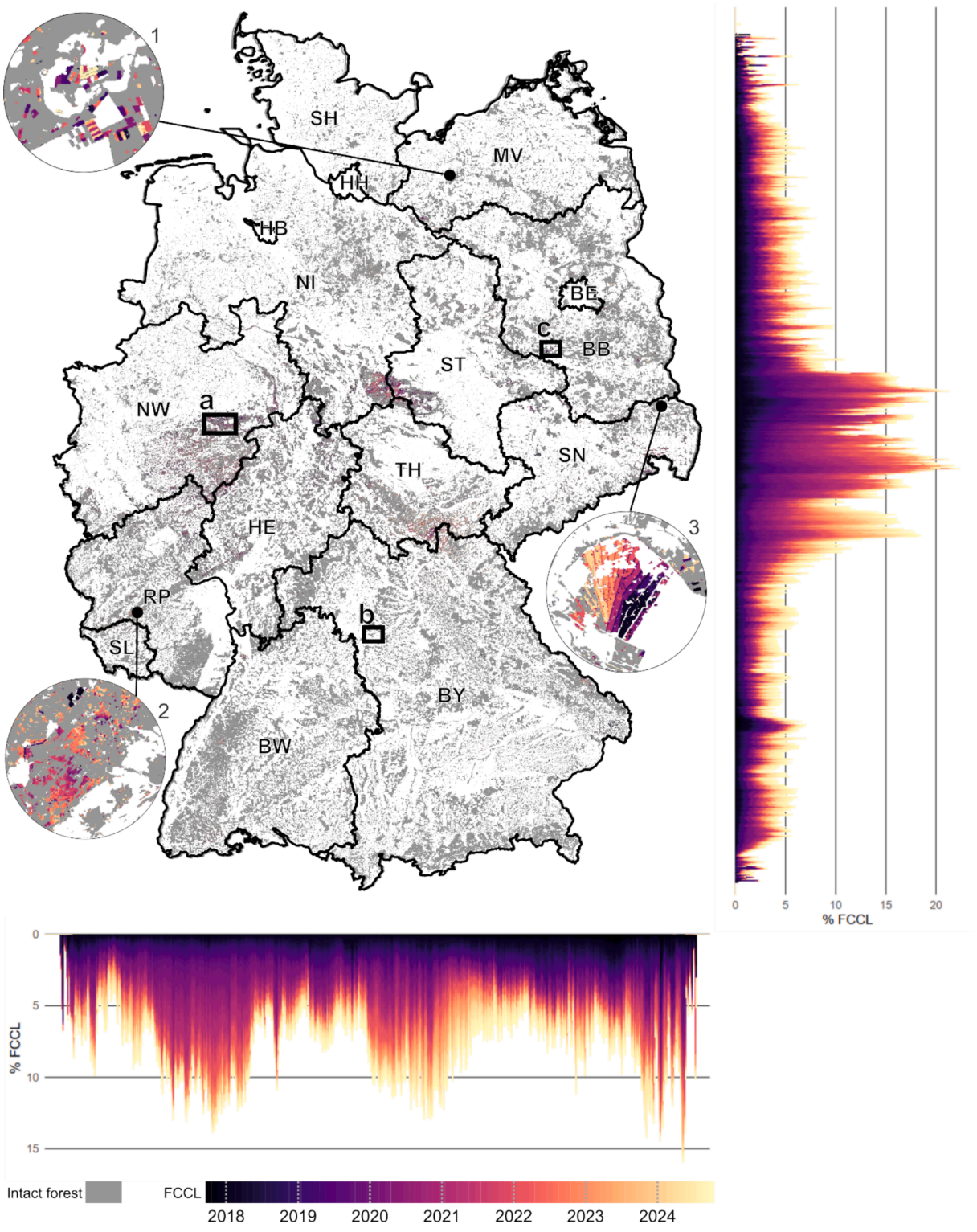

Fig. 1. FCCL in Germany across all forest types from September 2017 – September 2024. Marginal plots show the FCCL percentage of the total forest area per stripe of 1 km width or height, respectively. Zoom-ins of 1) regular harvest, 2) bark beetle and partial salvage logging, 3) clear-cuts to prepare land for open pit mining. Federal states: HH = Hamburg, BE = Berlin, HB = Bremen, SH = Schleswig-Holstein, BW = Baden-Württemberg, BY = Bavaria, MV = Mecklenburg-Western Pomerania, SL = Saarland, BB = Brandenburg, RP = Rhineland Palatinate, NI = Lower Saxony, HE = Hesse, SN = Saxony, ST = Saxony-Anhalt, TH = Thuringia, NW = North Rhine-Westphalia. The locations of a, b, and c refer to Fig. 9.

(dem_max), and minimum elevation (elev_min). Regarding IncNodePurity, fi_proz is followed by the forest area in percent (wald_proz), the 90% percentile of the climatic water balance per year (kwbj_max), the 90% percentile of the mean July temperature (tjul_max), the mean value of the climatic water balance in the year (kwbj_mit), and the 90% percentile of the temperature difference between the coldest and warmest month (tempvar_max).

The random forest model explains ~ 39% of the variance in FCCL,

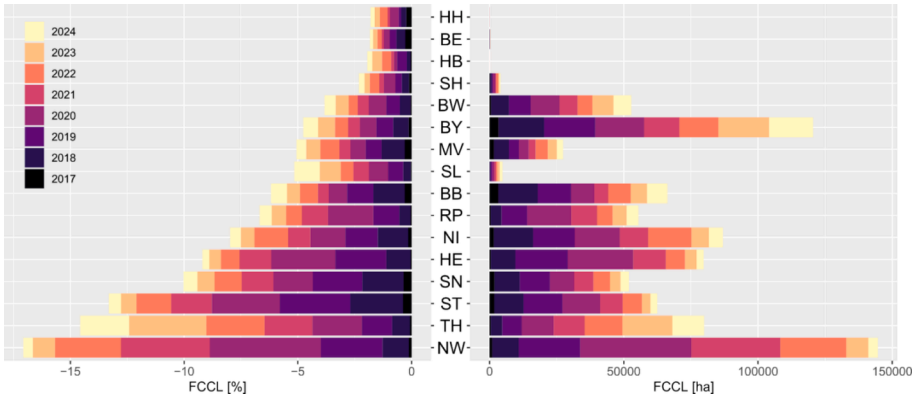

Fig. 2. FCCL across all forest types aggregated to annual sums at federal state level, expressed as FCCL area shares (in percent, left) and absolute loss areas (in hectare, right). Note: 2017 and 2024 are limited to September-December and January-June, respectively. Ordering is according to the FCCL percentage. Locations of the federal states are shown in Fig. 1.

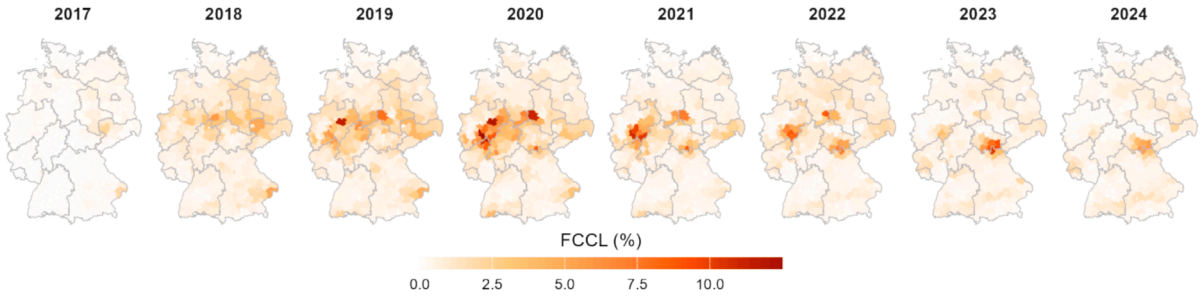

Fig. 3. Annual FCCL across all forest types at district level for 2017–2024. Note that 2017 and 2024 include only September-December and January-June, respectively.

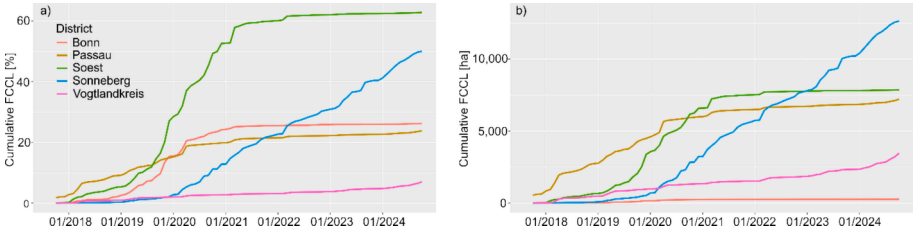

Fig. 4. FCCL of coniferous forests of selected districts with distinct temporal patterns, a) cumulated percentages (with respect to coniferous forest area), b) cumulated area in hectares.

with an OOB RMSE of ~ 5.9%. While this indicates moderate predictive power, it is sufficient to identify the dominant factors shaping regional FCCL patterns, particularly the strong susceptibility of spruce forests. At the same time, the relatively low explained variance shows that the model is not suitable for precise predictions, as major drivers such as storms, droughts, and heatwaves are not directly captured by the static environmental predictors. Nevertheless, the results clearly demonstrate that regions with high spruce cover are especially prone to FCCL.

Consistent with these findings, spruce forests were the most affected by recent disturbances (2025). We computed spruce forest share in equal-sized hexagons covering Germany and the corresponding FCCL in spruce forests (Fig. 6). The bivariate map shows spruce cover (cyan = low cover, green = full cover) versus FCCL (dark blue = high losses in low-cover areas; red = high losses in high-cover areas). Northern Germany generally has a low share of spruce forests, but vast spruce areas were lost over the past years. The northern-most low mountain ranges such as Harz, Rhenish Massif, Saxon-Bohemian Chalk Sandstone Region and Thuringian Forest had high initial spruce shares but experienced substantial FCCL over the past years, while southern Germany shows comparatively low losses in spruce.

Fig. 7 summarizes spruce forest area and FCCL by federal state. Bavaria and Baden-Württemberg have the largest spruce forest areas (1.3 Mio ha and 377,000 ha, respectively), followed by North Rhine-Westphalia, Thuringia and Saxony (~ 200,000–250,000 ha each). The brown bars in Fig. 7 correspond to the FCCL area of spruce per federal state. The FCCL area in spruce forests is highest in North Rhine-Westphalia (114,000 ha), Bavaria (97,000 ha) and Thuringia (74,000 ha). Relative losses differ: in Bavaria, 7.4% of spruce forests were affected, whereas in Saxony-Anhalt 28,000 ha correspond to 67.3% of its spruce forests. Several states lost more than one quarter of their spruce forests, with the highest relative losses in Brandenburg (49.0%), North Rhine-Westphalia (47.3%), and Saarland (40.3%). The Ore Mountains in Saxony and the low mountain ranges in Baden-Württemberg and Bavaria retain the largest remaining spruce forests, i.e., those least affected by recent FCCL.

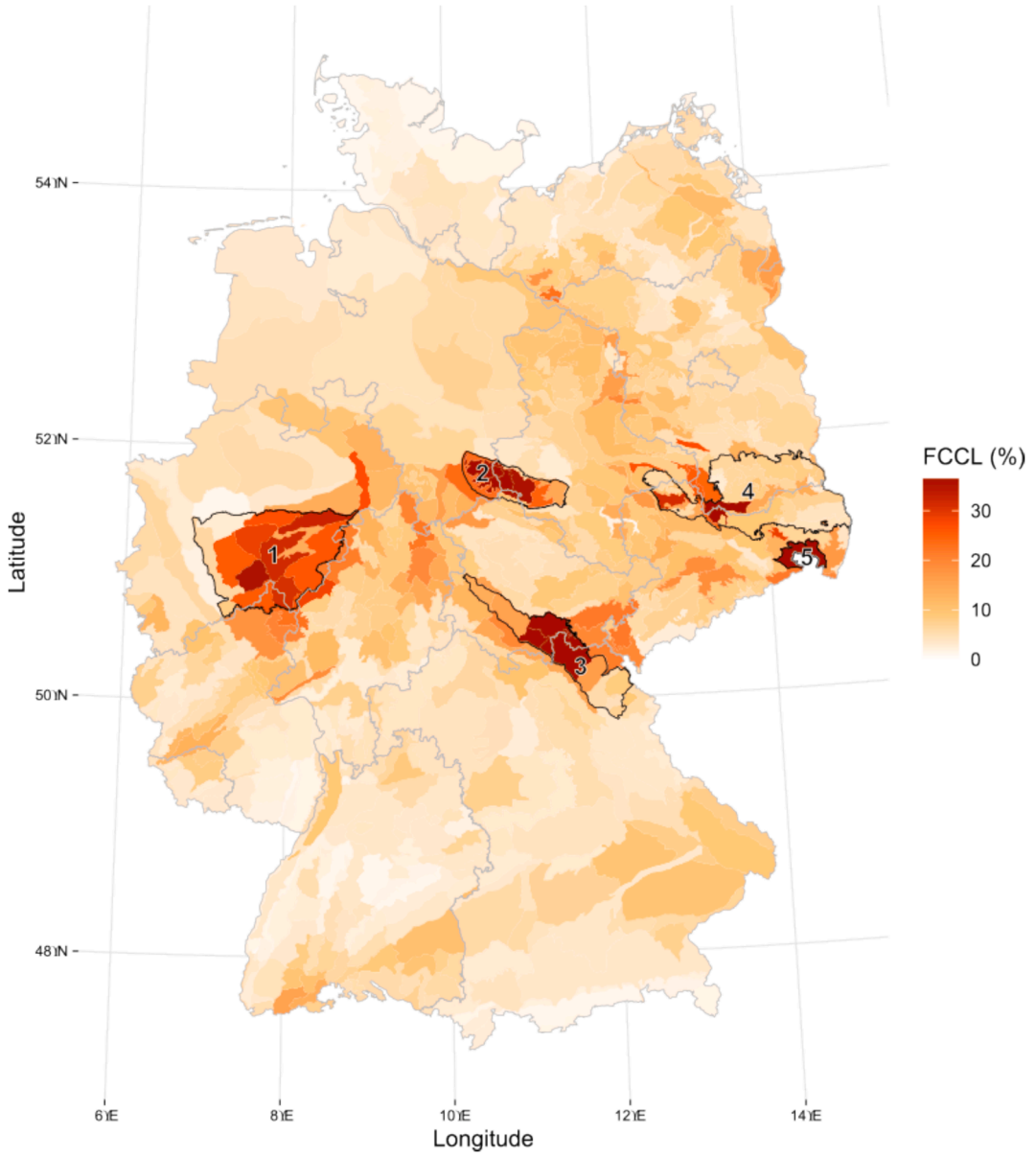

Fig. 5. FCCL across all forest types and aggregated from September 2017 – June 2024 at the level of forest growth districts. Federal state borders are shown in grey for better orientation. The numbers refer to forest growth regions that contain forest growth districts with high FCCL percentages and that are referred to in the text. 1 = Bergisches Land/Sauerland, 2 = Harz, 3 = Thüringer Gebirge/Frankenwald, 4 = Düben-Niederlausitzer Altmoränenland, 5 = Oberlausitzer Bergland.

3.5. Benefits from increased temporal resolution

Fig. 8 shows examples of FCCL from different regions in Germany. The first example (a, left column) is located in the Rhenish Massif in North Rhine-Westphalia in western Germany and shows a complex of drought, bark beetle, and salvage logging, which is typical for the period under consideration. The second example (b, center column) shows coppice in oak forests of Franconia (Bavaria), a traditional forest management practise rarely applied today. The third example (c, right column) shows several fires that took place in 2018, 2019, and 2022 near the municipality of Treuenbrietzen (Brandenburg). A comparison between the monthly and yearly color scales highlights the greater informational richness of the monthly plots, which capture gradual spatial expansion of FCCL areas. The seasonal color scale, in which losses from the same month are displayed in identical colors regardless of the year, provides additional information over the yearly product.

Seasonal patterns become evident: coppice, a planned forest management activity, predominantly occurs during the winter months, when access to the forests causes least impact on the soils and the wood moisture content is lowest (b). In contrast, forest fires in central Europe mainly occur during the summer months, when hot temperatures and dry conditions favor the spread of fires (c). The third example (a), however, is more complex. Most of the recorded FCCL originates from spruce forests, and losses appear in both summer and winter seasons. The FCCL recorded in summer likely reflects standing deadwood and advanced stages of bark beetle infestation, while FCCL in winter is associated with salvage logging and the removal of standing dead trees following such outbreaks.

The plot of cumulated FCCL areas by month reveals that most of the loss areas were recorded in winter with a peak in Febuary and March and a secondary peak in August and September (Fig. 9). In fact, two thirds of the FCCL areas were recorded from November to April. Fig. 9 shows the averages per month from September 2017 – June 2024 and the data range per month. It can be seen that the data range is large, particularly in winter, indicating the importance of large storm events and exceptional salvage logging for the total FCCL area. The spatial pattern of

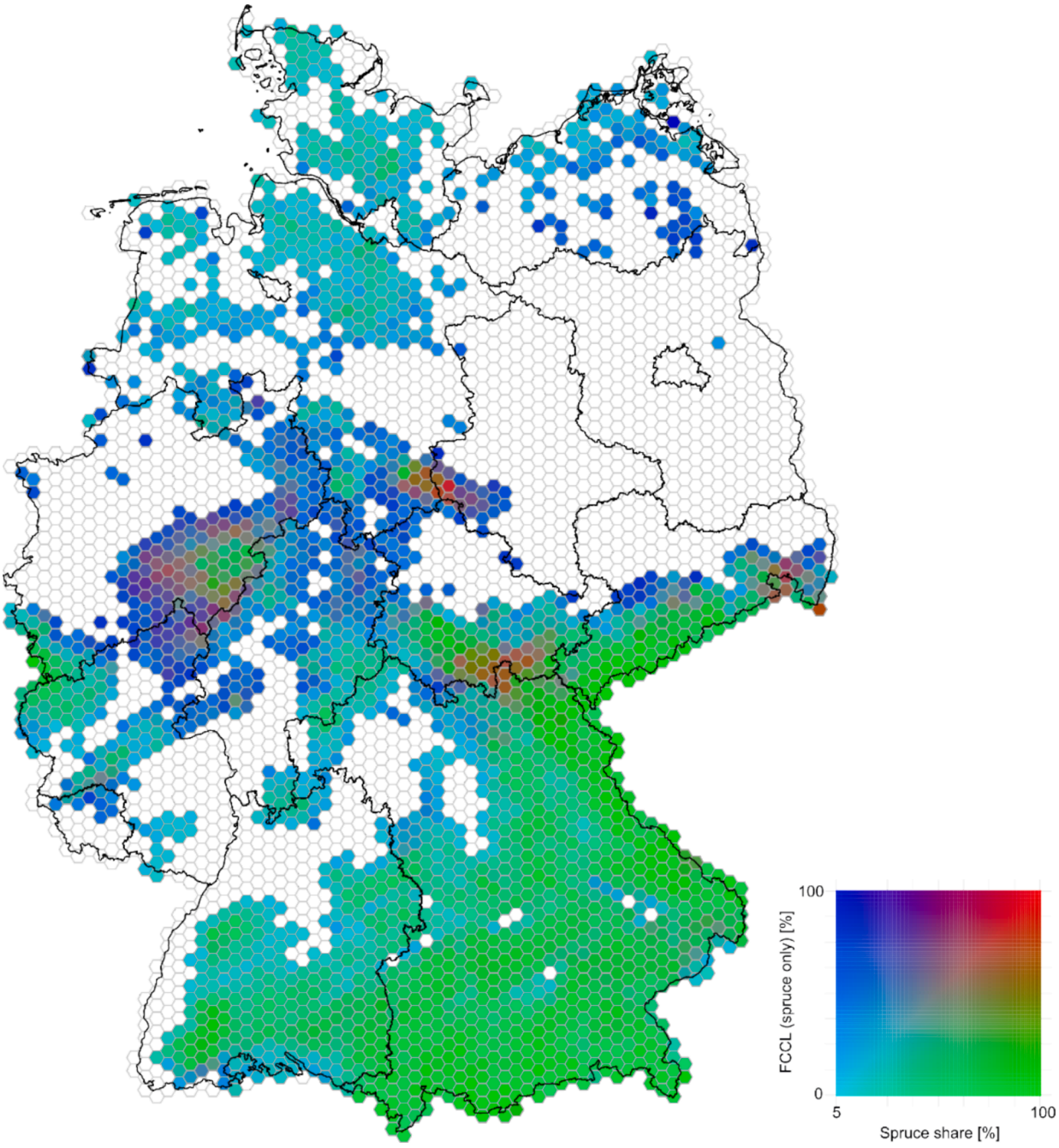

Fig. 6. Bivariate plot of spruce forest share based on the dominant tree species map by Blickensdörfer et al 2024 and FCCL in spruce forests only. Hexagons with < 5% spruce cover are shown in white.

seasonal FCCL at district level is shown in Appendix D.

4. Discussion

4.1. Quality assessment

Using a fully independent dataset, the validation confirms a robust performance of the proposed FCCL mapping approach. These results are comparable to previous studies, e.g. Mermoz et al. (2024) report 0.99 UA and 0.81 PA for the detection of clear-cuts in temperate forests in France; Reinosch et al. (2024) report 0.84 ± 0.02 UA and 0.85 ± 0.03 PA for 2018–2022 for the detection of disturbances in Germany. However, it should be noted that the reference data used here cover a period in the middle of the FCCL time series. The most recent time steps are typically more error-prone and challenging to validate. Nevertheless, due to almost levelled seasonality of the DI in coniferous forests, we assume even late FCCL detections to be reliable. In deciduous forests, seasonality of the DI is also small, but early wilting at a few locations can result in false positives.

Validation of clearly timed events such as fires or windthrows is often straightforward when the events attract the attention of the media. We found a number of examples where timing of the FCCL detection associated with such an event is within only one month, sometimes two months. When the event occurs at the beginning of a month, the method is capable of mapping the exact month. However, small-scale events – e.g., windthrows of only a few trees – are difficult to detect and more so to validate because they are often not reported. But even larger events often lack spatially explicit validation data.

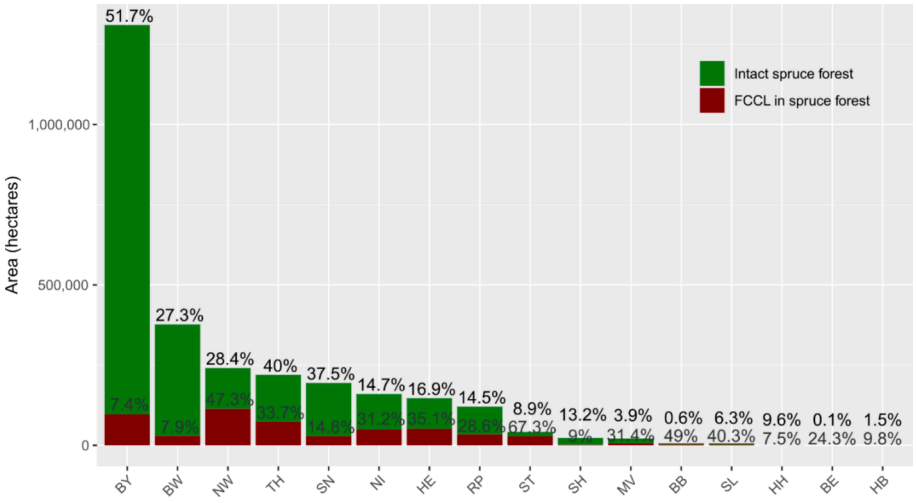

Fig. 7. Spruce forest area and FCCL area in spruce forests in hectares per federal state. Numbers reflect the corresponding percentages of spruce forests relative to the total forest area and the share of FCCL relative to the spruce forest area, respectively.

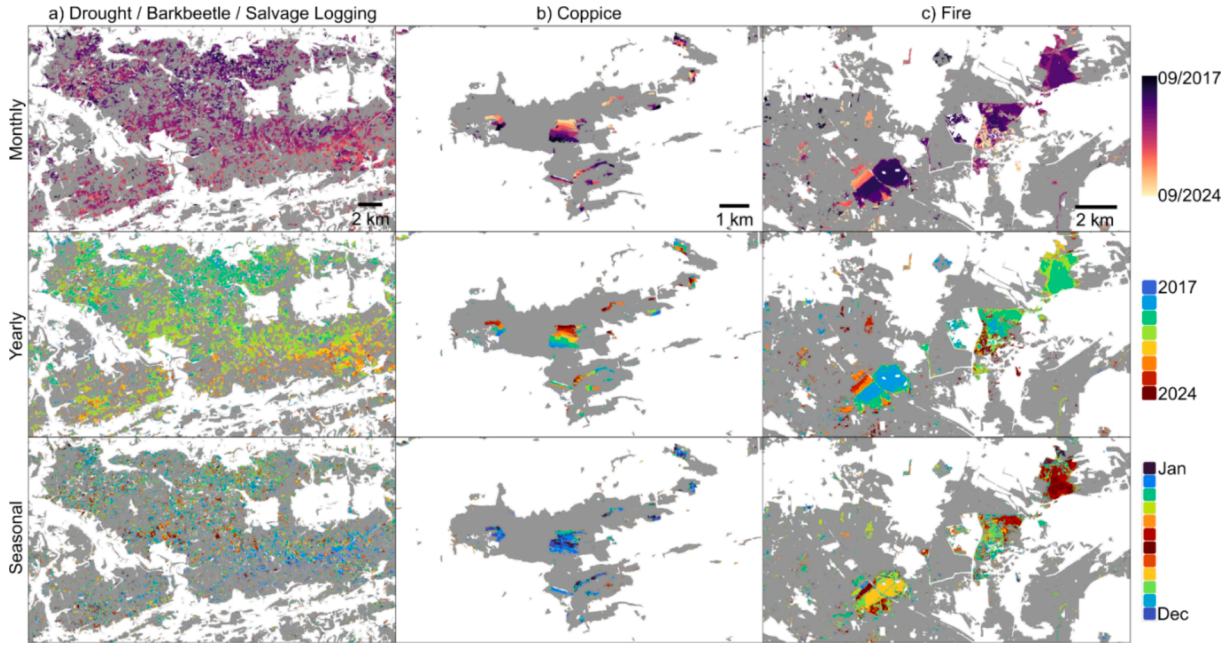

Fig. 8. Examples of FCCL visualized with monthly (top row), yearly (center row) and seasonal (bottom row) color scale. The columns show a complex of drought, bark beetle and salvage logging in western Germany near Arnsberg (a), coppice in Franconia near Bad Windsheim (b), and fire in Eastern Germany near Treuenbrietzen (c). The locations are indicated in Fig. 1. The reader is referred to the online platform https://eowald.dlr.de/ for an interactive exploration of the maps.

The relatively high spatial resolution of our product (10 m) is well suited to detect patches of FCCL. However, with our approach we are not able to detect FCCL of single trees, paricularly scattered standing deadwood. There is evidence that these contribute substantially to the canopy cover loss (Cheng et al., 2024). In addition, Schiefer et al. (2024) found that tree mortality was underestimated in Hansen et al. (2013) and Thonfeld et al. (2022) although general patterns were in line with their findings. As the approach presented here is similar to that in Thonfeld et al. (2022), we assume also underestimation of tree mortality in this study. However, most of the disturbance drivers do not ultimately result in standing deadwood. Often, patches that experienced a disturbance like a windthrow are cleared to prevent the spread of insects, which is e.g. part of bark beetle management. This may result in spectral signatures very similar to those of regular harvest. Another source of error is the underlying forest mask, particularly along forest edges.

4.2. Temporal resolution

There exists a variety of national (e.g., Lange et al., 2024) and continental (e.g., Buras et al., 2021; Viana-Soto and Senf, 2025) to global (Hansen et al., 2013) scale EO-based products related to forest condition and disturbance. However, none of them quantifies FCCL at monthly intervals and also off-season, even though common silvicultural practise in Germany recommends access to forests in winter when soils are frozen and therefore least damaged by heavy machinery. We could demonstrate the use of monthly, full-year data as it allows to allocate FCCL in space and time. The reasons for the dominance of FCCL winter detections can be large winter storm events (e.g., “Friederike” in January 2018) – winter sorms are typical for central Europe –, and sanitary logging as well as planned harvest intentionally placed in winter months. Fire and insect infestations, on the other hand, typically occur in summer. Therefore, we see high potential of our data to characterize

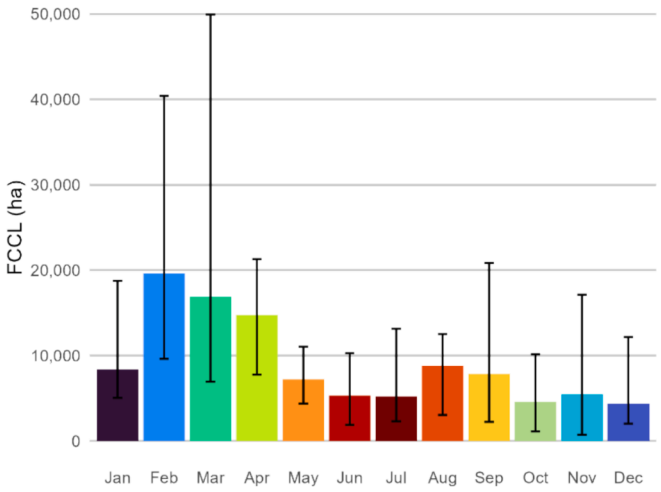

Fig. 9. Seasonal FCCL records, i.e. monthly information irrespective of year. Colored bars represent averages, with maxima and minima of each month in the observation period overlaid as black bars. Colors are identical to the color legend of the seasonal presentation (bottom row) in Fig. 8.

and differentiate disturbance drivers.

Our methodology is robust towards outliers as we filter the time series and apply compositing. Depending on cloud and snow cover and illumination conditions, hence also depending on topography, the resulting monthly time series may still contain gaps. Although the majority of gaps can be expected during the winter season, we recorded most FCCL between November and April. For accurate temporal allocation of FCCL, we recommend including the winter season, which is usually not considered in methods that rely on phenology (e.g., Lange et al., 2024).

Our approach and its high temporal resolution offers new insights into forest disturbance dynamics which help better understanding of forest mortality (Hartmann et al., 2018).

4.3. Recent FCCL dynamics and the consequences

The shifting hotspot patterns point to interacting disturbance mechanisms, including storm legacy effects, delayed drought-induced mortality, and bark beetle population dynamics.

The FCCL product presented here quantifies only losses of canopy cover, without considering recovery. Previous studies have applied EO techniques to monitor forest regrowth (Kennedy et al., 2010; White et al., 2017), and there is evidence of recovery even after relatively short time (Mandl et al., 2024; Seidl et al., 2024). However, while some structural attributes indicate a very early trend back to pre-disturbance levels (Kacic et al., 2023) – e.g., canopy cover increasing after a severe decline due to a clear-cut – it is challenging to uncover whether this is driven by the growth of small trees or the expansion of tall grasses and shrubs. For this reason, regrowth was not included in the present study.

FCCL due to land use changes (e.g. open pit mining, settlement expansion, road construction) exists in Germany but currently represents a small fraction of total FCCL.

Losses of 7% to over 60% of coniferous forest cover at the district level are likely to have severe impacts on forest management and multiple forest-related ecosystem services. These include regulating services such as water retention, soil erosion protection, and water quality (Winter et al., 2025), as well as economic services related to timber supply and market dynamics (Spathelf et al., 2022). Cultural and recreational services are affected, and changes in forest structure can influence local microclimate, including landscape cooling and precipitation patterns (Blumröder et al., 2021; Grieger et al., 2025). Furthermore, structural changes associated with FCCL (Kacic et al., 2023) increase forest fragmentation (Coleman and Kuenzer, 2025), with cascading effects on biodiversity (Graser et al., 2024).

4.4. The role of spruce forests

The strong association between FCCL and spruce-dominated forests highlights long-term structural vulnerabilities of even-aged spruce stands under increasing climatic stress. While the relationship is statistical rather than causal, it aligns with the observation that most of the recent canopy cover losses in Germany occurred in spruce forests (2024; Bolte et al., 2025). Not only the most recent invetory indicates a decline in spruce cover, but also the annual crown condition assessments (2025). High proportions of even-aged spruce monocultures correspond to elevated FCCL risk. At the same time, Fig. 6 and Fig. 7 show that some regions with extensive spruce cover, such as the Ore Mountains, experienced relatively low FCCL until recently, though losses have increased in the past 24 months, indicating areas at high near-future risk. Even though virtually all tree species are affected by the droughts since 2018, spruce – the economically most important tree species in Germany – has suffered severe declines, largely due to bark beetle calamities exacerbated by drought and heat since 2018 (Bolte et al., 2025). While latest scientific findings recommend reconsideration of previous management strategies (Hlásny et al., 2021), there is still need for better understanding of the drivers of bark beetle populations (Biedermann et al., 2019). However, the joint occurrence of drought and heat – which is expected to increase with climate change – will intensify and extend the emergence of spruce bark beetle mass outbreaks (Potterf et al., 2025). Early detection of bark beetle calamities via remote sensing remains challenging (Abdullah et al., 2019, 2018; Bárta et al., 2021; Holzwarth et al., 2020; König et al., 2023), but detection of later stages (standing deadwood or post-logging) is reliable (Schiefer et al., 2024; Schiller et al., 2024, 2024; Thonfeld et al., 2022). Timely detection of bark beetle outbreak hotspots and overseen disturbance areas is therefore critical for forest management.

5. Conclusions

We monitored forest canopy cover loss (FCCL) dynamics in Germany at 10 m spatial resolution and monthly intervals from September 2017 to September 2024, achieving an OA of 0.92. We detected a total of 924.000 ha of FCCL, roughly equivalent to the size of Cyprus. The high resolution and full-season coverage allow detailed characterization of spatio-temporal patterns, precise allocation of canopy cover losses, and improved understanding of underlying processes. The FCCL dataset includes both human-induced disturbances (e.g., planned harvest, land use changes, mining, infrastructure) and natural disturbances (e.g., drought, heatwaves, insect infestations, windthrow, fire), without explicitly specifying them. In line with objective i), we implemented an improved forest mask, modified anomaly detection, and computed additional features to support the analysis.

Widespread FCCL occurred in northern Germany in early 2018, mainly due to large storm events, followed by drought- and heat-induced losses cascading with insect infestations, peaking in 2020. Since then, FCCL rates have generally declined but remain high in some regions. Regarding objective ii), hotspots shifted over time from northeastern to western Germany and subsequently to central eastern Germany. Some districts in Thuringia, Saxony, Bavaria, and Saarland show increasing FCCL in recent years at regional level.

With respect to objective iii), regions with a high share of still-intact spruce forests, particularly the Ore Mountains (Saxony), Bavaria, and Baden-Württemberg, have high potential for near-future FCCL. Although spruce mortality depends on numerous factors, the species is susceptible to the consequences of climate warming. Spruce forests will likely suffer under continued droughts and heatwaves. This poses challenges to forest management as most of the spruce forests in Germany are located outside their ecological niche. The consequences of further large-scale disturbances in spruce forests have severe impacts on

the forest sector as well as many other ecosystem services. The conversion from homogeneous spruce stands to climate-adapted mixed forests consisting of climate-adapted tree species should be accompanied by area-wide monitoring, including EO technologies.

The monthly resolution and off-season mapping capability of our FCCL assessment are critical for accurately identifying disturbance events and improving attribution to specific drivers. Full-season coverage and high temporal resolution enhance the detection of abrupt events, such as windstorms. While Sentinel-2 provides the majority of data, the inclusion of Landsat increases data availability and reduces gaps. To our knowledge, this approach is the first to account for winter acquisitions, confirming that a substantial portion of FCCL occurs in winter. These results demonstrate that year-round monitoring is essential to fully exploit EO capabilities for forest disturbance detection.

CRediT authorship contribution statement

Frank Thonfeld: Writing – original draft, Visualization, Methodology, Investigation, Formal analysis, Conceptualization. **Patrick Kacic:** Writing – review & editing, Formal analysis, Data curation. **Stefanie Holzwarth:** Writing – review & editing, Investigation. **Marco Wegler:** Writing – review & editing, Validation. **Sarah Asam:** Writing – review & editing, Visualization. **Claudia Kuenzer:** Writing – review & editing, Visualization, Supervision.

Declaration of competing interest

The authors declare that they have no known competing financial interests or personal relationships that could have appeared to influence the work reported in this paper.

Acknowledgements

This Research was conducted within the ForstEO project (FKZ 2220WK81A4), funded by the Federal Ministry of Agriculture, Food and Regional Identity and the Federal Ministry for the Environment, Climate Action, Nature Conservation and Nuclear Safety based on a decision of the German Bundestag from Waldklimafonds through the Fachagentur Nachwachsende Rohstoffe e.V. (FNR). PK acknowledges funding from the DFG (Deutsche Forschungsgemeinschaft) within the framework of the Research Unit BETA-FOR (Enhancing the structural diversity between patches for improving multidiversity and multifunctionality in production forests) (grant no. FOR 5375/1, project number 459717468). The authors gratefully acknowledge the computational and data resources provided through the joint high-performance data analytics (HPDA) project “terrabyte” of the German Aerospace Center (DLR) and the Leibniz Supercomputing Center (LRZ).

Appendix A

Attributes of the forest growth district dataset. Entries in italics were removed from analysis.

Data field	Description
gid	*Technical primary key*
wg_bu	*Nationwide ID of the growing region (as of 2011)*
wb_bu	*Nationwide ID of the growth district (as of 2011)*
bez_wg_bu	*Nationwide designation of the growth area (as of 2011)*
bez_wb_bu	*Nationwide designation of the growth district (as of 2011)*
gesfl_ha	*Total area in ha*
wfl_ha	*Forest area in ha (gesfl_ha * (wald_proz / 100))*
wald_proz	Forest area in per cent
lb_proz	Deciduous trees in % of the forest area
nb_proz	Conifers in % of the forest area
bu_proz	Beech in % of the forest area
ei_proz	Oak in % of the forest area
slb_proz	Other deciduous trees in % of the forest area
fi_proz	Spruce in % of the forest area
ki_proz	Pine in % of the forest area
snb_proz	Other conifers in % of the forest area
m_ueber_nn	Altitude zone above sea level
tempj_min	10% percentile of the mean annual temperature [degrees Celsius]
tempj_mit	Mean value of the mean annual temperature [degrees Celsius]
tempj_max	90% percentile of the annual mean temperature [degrees Celsius]
tempv_min	10% percentile of the mean temperature in the forest vegetation period (May − Sept.) [degrees Celsius]
tempv_mit	Mean value of the mean temperature in the forest growing season (May − Sept.) [degrees Celsius]
tempv_max	90% percentile of the mean temperature in the forest growing season (May − Sept.) [degrees Celsius]
dt10_min	10% percentile of the sum of days with a mean temperature of 10 degrees Celsius and more
dt10_mit	Mean value of the sum of days with a mean temperature of 10 degrees Celsius and above
dt10_max	90% percentile of the sum of days with an average temperature of 10 degrees Celsius and more
tempvar_min	10% percentile of the temperature difference between the coldest and warmest month [degrees Kelvin]
tempvar_mit	Mean value of the temperature difference between the coldest and warmest month [degrees Kelvin]
tempvar_max	90% percentile of the temperature difference between the coldest and warmest month [degrees Kelvin]
tjan_min	10% percentile of the mean January temperature [degrees Celsius]
tjan_mit	Mean value of the mean January temperature [degrees Celsius]
tjan_max	90% percentile of the mean January temperature [degrees Celsius]
tjul_min	10% percentile of the mean July temperature [degrees Celsius]
tjul_mit	Mean value of the mean July temperature [degrees Celsius]
tjul_max	90% percentile of the mean July temperature [degrees Celsius].
prev_min	10% percentile of the mean precipitation in the forest vegetation period (May − Sept.) [mm]
prev_mit	Mean value of the mean precipitation in the forest growing season (May − Sept.) [mm]
prev_max	90% percentile of the mean precipitation in the forest growing season (May − Sept.) [mm]
prej_min	10% percentile of the mean annual precipitation [mm]

(*continued on next page*)

(*continued*)

Data field	Description
prej_mit	Mean value of the mean annual precipitation [mm]
prej_max	90% percentile of the mean annual precipitation [mm]
dem_min	10% percentile of the thermo-hygric index according to De Martonne
dem_mit	Mean value of the thermo-hygric index according to De Martonne
dem_max	90% percentile of the thermo-hygric index according to De Martonne
kwbv_min	10% percentile of the climatic water balance in the forest vegetation period (May – Sept.) [mm]
kwbv_mit	Mean value of the climatic water balance in the forest growing season (May – Sept.) [mm]
kwbv_max	90% percentile of the climatic water balance in the forest growing season (May – Sept.) [mm]
kwbj_min	10% percentile of the climatic water balance in the year [mm]
kwbj_mit	Mean value of the climatic water balance in the year [mm]
kwbj_max	90% percentile of the climatic water balance per year [mm]
the_geom	*Geometry column*

Appendix B

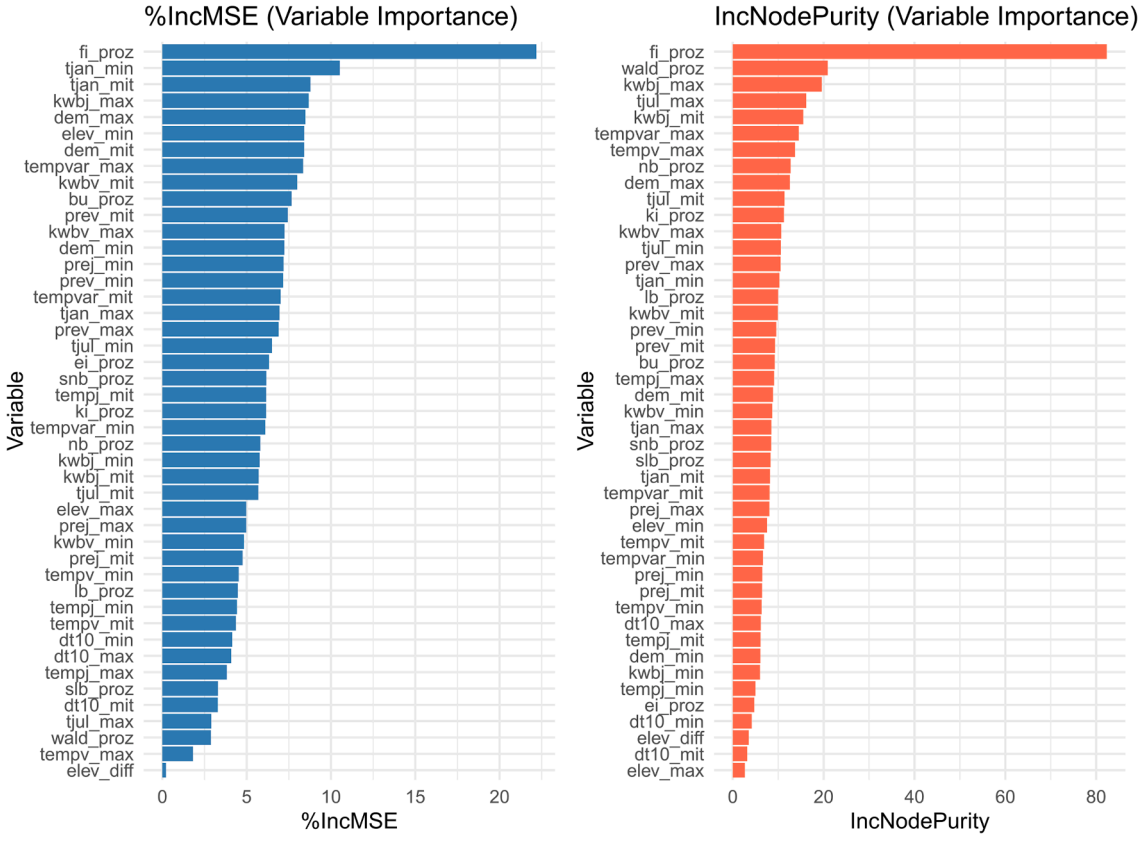

Variable importance of the random forest regression between environmental variables and FCCL of all forest types.

Appendix C

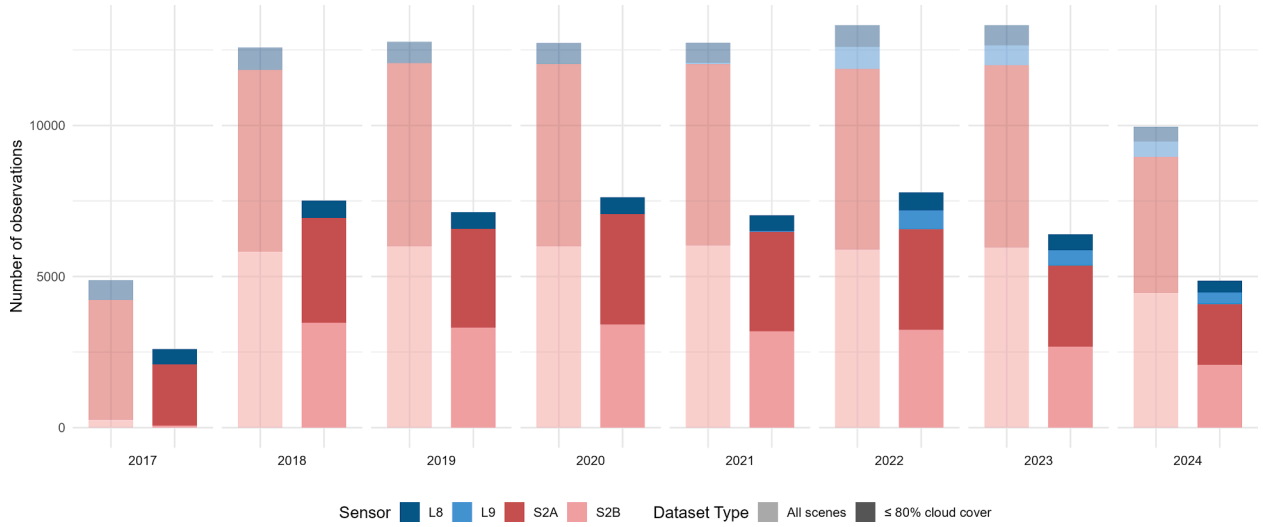

Number of available (transparent) and processed (≤80% cloud cover) images per year and sensor (2017–2024). Of 92,000 scenes, ~51,000 were used, including ~ 45,000 from Sentinel-2. Fewer scenes were available in 2017 as only Sentinel-2A and Landsat-8 were operational. Note: 2024 includes nine months only.

Appendix D

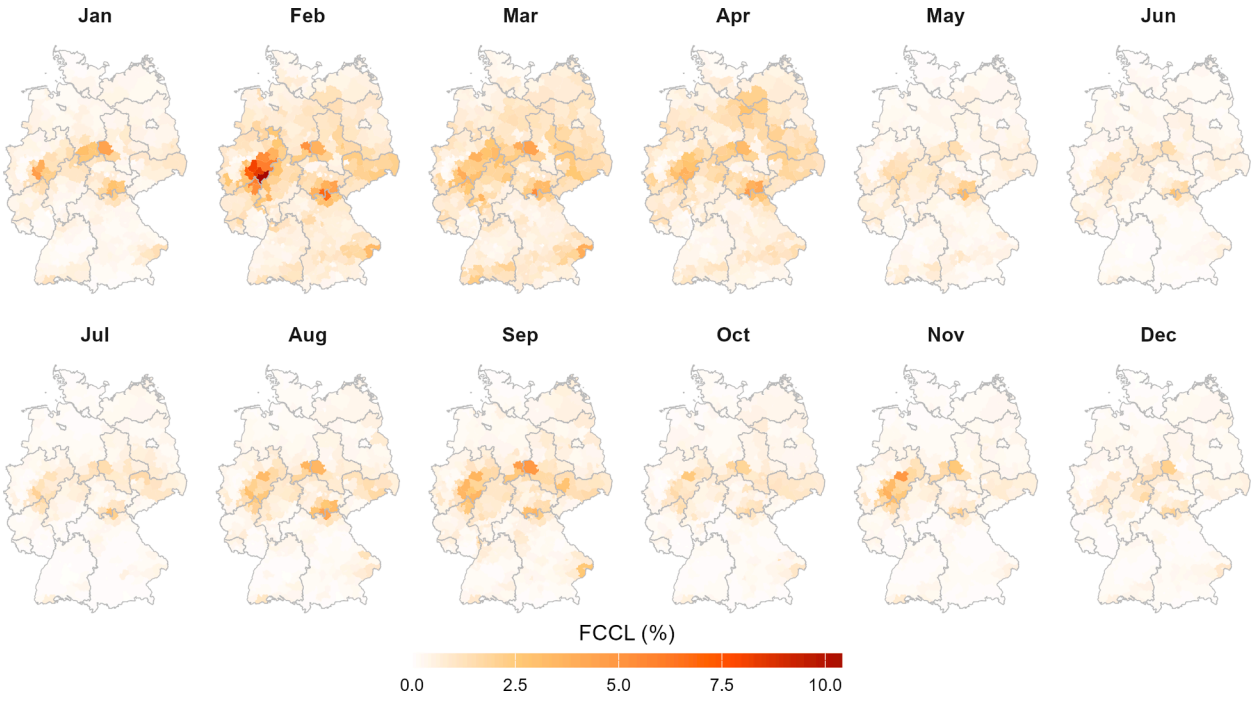

Cumulative forest canopy cover loss (FCCL) per month across all years, aggregated by district. Federal state borders are shown for better orientation.

Data availability

The FCCL raster dataset (https://doi.org/10.15489/ef9wwc5sff75) as well as the aggregated results at administrative units (https://doi.org/10.15489/jctru9ze1t42) are available on DLR's EOC geoservice (https://geoservice.dlr.de/web/datasets/fccl, https://geoservice.dlr.de/web/datasets/fccl_stats). A client for interactive visualisation is available under https://eowald.dlr.de/.

References

Abdullah, H., Darvishzadeh, R., Skidmore, A.K., Groen, T.A., Heurich, M., 2018. European spruce bark beetle (Ips typographus, L.) green attack affects foliar reflectance and biochemical properties. Int. J. Appl. Earth Obs. Geoinf. 64, 199–209. https://doi.org/10.1016/j.jag.2017.09.009.

Abdullah, H., Darvishzadeh, R., Skidmore, A.K., Heurich, M., 2019. Sensitivity of Landsat-8 OLI and TIRS Data to foliar properties of early stage bark beetle (Ips typographus, L.) infestation. Remote Sens. (Basel) 11, 398. https://doi.org/10.3390/rs11040398.

Arthur, G., Jonathan, L., Juliette, C., Nicolas, L., Christian, P., Hugues, C., 2024. Spatial and remote sensing monitoring shows the end of the bark beetle outbreak on Belgian and north-eastern France Norway spruce (*Picea abies*) stands. Environ. Monit. Assess. 196, 226. https://doi.org/10.1007/s10661-024-12372-0.

Bárta, V., Lukeš, P., Homolová, L., 2021. Early detection of bark beetle infestation in Norway spruce forests of Central Europe using Sentinel-2. Int. J. Appl. Earth Obs. Geoinf. 100, 102335. https://doi.org/10.1016/j.jag.2021.102335.

Biedermann, P.H.W., Müller, J., Grégoire, J.-C., Gruppe, A., Hagge, J., Hammerbacher, A., Hofstetter, R.W., Kandasamy, D., Kolarik, M., Kostovcik, M., Krokene, P., Sallé, A., Six, D.L., Turrini, T., Vanderpool, D., Wingfield, M.J., Bässler, C., 2019. Bark beetle population dynamics in the anthropocene: challenges and solutions. Trends Ecol. Evol. 34, 914–924. https://doi.org/10.1016/j.tree.2019.06.002.

BKG, 2025. Verwaltungsgebiete 1:250 000. Data as of 01.01.2024. https://www.bkg.bund.de.

Blickensdörfer, L., Oehmichen, K., Pflugmacher, D., Kleinschmit, B., Hostert, P., 2024. National tree species mapping using Sentinel-1/2 time series and German National Forest Inventory data. Remote Sens. Environ. 304, 114069. https://doi.org/10.1016/j.rse.2024.114069.

Blumröder, J.S., May, F., Härdtle, W., Ibisch, P.L., 2021. Forestry contributed to warming of forest ecosystems in northern Germany during the extreme summers of 2018 and 2019. Ecol. Solutions Evidence 2, e12087. https://doi.org/10.1002/2688-8319.12087.

2024 2024, Deutschland - Ausgewählte Ergebnisse der vierten Bundeswaldinventur. 60 . Der Wald .

BMLEH (Ed.), 2025. Ergebnisse der Waldzustandserhebung 2024. 80 pages.

Bolte, A., Riedel, T., Rock, J., Kroiher, F., Dunger, K., 2025. Fichte verliert erhebliche Anteile, Kiefer ist häufigste Baumart. proWALD 2, 4–7.

Breiman, L., 2001. Random forests. Mach. Learn. 45, 5–32. https://doi.org/10.1023/A:1010933404324.

Brun, P., Psomas, A., Ginzler, C., Thuiller, W., Zappa, M., Zimmermann, N.E., 2020. Large-scale early-wilting response of Central European forests to the 2018 extreme drought. Glob. Chang. Biol. 26, 7021–7035. https://doi.org/10.1111/gcb.15360.

Buras, A., Rammig, A., Zang, C.S., 2021. The European Forest Condition Monitor: Using Remotely Sensed Forest Greenness to Identify Hot Spots of Forest Decline. Frontiers in Plant Science 12.

Cheng, Y., Oehmcke, S., Brandt, M., Rosenthal, L., Das, A., Vrieling, A., Saatchi, S., Wagner, F., Mugabowindekwe, M., Verbruggen, W., Beier, C., Horion, S., 2024. Scattered tree death contributes to substantial forest loss in California. Nat. Commun. 15, 641. https://doi.org/10.1038/s41467-024-44991-z.

Coleman, K., Kuenzer, C., 2025. Forest fragmentation in bavaria: a first-time quantitative analysis based on earth observation data. Remote Sens. (Basel) 17, 2558. https://doi.org/10.3390/rs17152558.

de Brito, M.M., 2021. Compound and cascading drought impacts do not happen by chance: a proposal to quantify their relationships. Sci. Total Environ. 778, 146236. https://doi.org/10.1016/j.scitotenv.2021.146236.

Descals, A., Verger, A., Yin, G., Filella, I., Peñuelas, J., 2023. Widespread drought-induced leaf shedding and legacy effects on productivity in European deciduous forests. Remote Sens. Ecol. Conserv. 9, 76–89. https://doi.org/10.1002/rse2.296.

Gauer, J., Aldinger, E., 2005. Waldökologische Naturräume Deutschlands - Forstliche Wuchsgebiete und Wuchsbezirke - mit Karte 1:1.000.000, Mitteilungen des Vereins für Forstliche Standortskunde und Forstpflanzenzüchtung. HENKELdruck, Stuttgart.

Gauer, J., Kroiher, F. (Eds.), 2012. Waldökologische Naturräume Deutschlands: Forstliche Wuchsgebiete und Wuchsbezirke. Digitale Topographische Grundlagen - Neubearbeitung Stand 2011. Landbauforschung Sonderheft 359. Johann Heinrich von Thünen-Institut, Braunschweig.

Gnilke, A., Sanders, T.G.M., 2022. Distinguishing Abrupt and Gradual Forest Disturbances With MODIS-Based Phenological Anomaly Series. Frontiers in Plant Science 13.

Graser, A., Georg, M., Kallmayer, J., Marten, A., Pertl, C., Rumpf, H., Senf, C., Kamp, J., 2024. Large-scale forest disturbance and associated management shape bird communities in central European spruce forests. J. Appl. Ecol. N/a 1_15. https://doi.org/10.1111/1365-2664.14849.

Grieger, S., Kappas, M., Karel, S., Koal, P., Koukal, T., Löw, M., Zwanzig, M., Putzenlechner, B., 2025. Impact of forest disturbance derived from Sentinel-2 time series on Landsat 8/9 land surface temperature: the case of Norway spruce in Central Germany. ISPRS J. Photogramm. Remote Sens. 228, 388–407. https://doi.org/10.1016/j.isprsjprs.2025.07.006.

Hansen, M.C., Potapov, P.V., Moore, R., Hancher, M., Turubanova, S.A., Tyukavina, A., Thau, D., Stehman, S.V., Goetz, S.J., Loveland, T.R., Kommareddy, A., Egorov, A., Chini, L., Justice, C.O., Townshend, J.R.G., 2013. High-resolution global maps of 21st-century forest cover change. Science 342, 850–853. https://doi.org/10.1126/science.1244693.

Hartmann, H., Moura, C.F., Anderegg, W.R.L., Ruehr, N.K., Salmon, Y., Allen, C.D., Arndt, S.K., Breshears, D.D., Davi, H., Galbraith, D., Ruthrof, K.X., Wunder, J., Adams, H.D., Bloemen, J., Cailleret, M., Cobb, R., Gessler, A., Grams, T.E.E., Jansen, S., Kautz, M., Lloret, F., O'Brien, M., 2018. Research frontiers for improving our understanding of drought-induced tree and forest mortality. New Phytol. 218, 15–28. https://doi.org/10.1111/nph.15048.

Healey, S., Cohen, W., Zhiqiang, Y., Krankina, O., 2005. Comparison of Tasseled Cap-based Landsat data structures for use in forest disturbance detection. Remote Sens. Environ. 97, 301–310. https://doi.org/10.1016/j.rse.2005.05.009.

Hlásny, T., König, L., Krokene, P., Lindner, M., Montagné-Huck, C., Müller, J., Qin, H., Raffa, K.F., Schelhaas, M.-J., Svoboda, M., Viiri, H., Seidl, R., 2021a. Bark beetle outbreaks in europe: state of knowledge and ways forward for management. Curr Forestry Rep 7, 138–165. https://doi.org/10.1007/s40725-021-00142-x.

Hlásny, T., Zimová, S., Merganičová, K., Štěpánek, P., Modlinger, R., Turčáni, M., 2021b. Devastating outbreak of bark beetles in the Czech Republic: drivers, impacts, and management implications. For. Ecol. Manage. 490, 119075. https://doi.org/10.1016/j.foreco.2021.119075.

Holzwarth, S., Thonfeld, F., Abdullahi, S., Asam, S., Da Ponte Canova, E., Gessner, U., Huth, J., Kraus, T., Leutner, B., Kuenzer, C., 2020. Earth observation based monitoring of forests in Germany: a review. Remote Sens. (Basel) 12, 3570. https://doi.org/10.3390/rs12213570.

Holzwarth, S., Thonfeld, F., Kacic, P., Abdullahi, S., Asam, S., Coleman, K., Eisfelder, C., Gessner, U., Huth, J., Kraus, T., Shatto, C., Wessel, B., Kuenzer, C., 2023. Earth-observation-based monitoring of forests in germany—recent progress and research frontiers: a review. Remote Sens. (Basel) 15, 4234. https://doi.org/10.3390/rs15174234.

Kacic, P., Thonfeld, F., Gessner, U., Kuenzer, C., 2023. Forest Structure Characterization in Germany: novel products and analysis based on GEDI, Sentinel-1 and Sentinel-2 Data. Remote Sens. (Basel) 15, 1969. https://doi.org/10.3390/rs15081969.

Kennedy, R.E., Yang, Z., Cohen, W.B., 2010. Detecting trends in forest disturbance and recovery using yearly Landsat time series: 1. LandTrendr — temporal segmentation algorithms. Remote Sens. Environ. 114, 2897–2910. https://doi.org/10.1016/j.rse.2010.07.008.

Knapp, N., Wellbrock, N., Bielefeldt, J., Dühnelt, P., Hentschel, R., Bolte, A., 2024. From single trees to country-wide maps: modeling mortality rates in Germany based on the crown condition survey. For. Ecol. Manage. 568, 122081. https://doi.org/10.1016/j.foreco.2024.122081.

König, S., Thonfeld, F., Förster, M., Dubovyk, O., Heurich, M., 2023. Assessing combinations of landsat, sentinel-2 and sentinel-1 time series for detecting bark beetle infestations. Gisci. Remote Sens. 60, 2226515. https://doi.org/10.1080/15481603.2023.2226515.

Lange, M., Preidl, S., Reichmuth, A., Heurich, M., Doktor, D., 2024. A continuous tree species-specific reflectance anomaly index reveals declining forest condition between 2016 and 2022 in Germany. Remote Sens. Environ. 312, 114323. https://doi.org/10.1016/j.rse.2024.114323.

Langner, N., Oehmichen, K., Backa, J., Eisenecker, P., Reinosch, E., Wiesehahn, J., Hoffmann, K., Adler, P., Beckschäfer, P., 2024. Referenzdaten aus dem Projekt FNEWS. Johann Heinrich von Thünen Institut, DE. https://doi.org/10.3220/DATA20240111153336-0.

Langner, N., Oehmichen, K., Henning, L., Blickensdörfer, L., Riedel, T., 2022. Bestockte Holzbodenkarte 2018. Johann Heinrich von Thünen-Institut, DE. https://doi.org/10.3220/DATA20221205151218.

Li, J., Roy, D.P., 2017. A Global analysis of sentinel-2A, sentinel-2B and Landsat-8 data revisit intervals and implications for terrestrial monitoring. Remote Sens. (Basel) 9, 902. https://doi.org/10.3390/rs9090902.

Liaw, A., Wiener, M., 2002. Classification and Regression by randomForest. R News, 2 (3), 18-22. https://CRAN.R-project.org/doc/Rnews/.

Mack, P., Kremer, J., Kleinschmit, D., 2023. Forest dieback reframed and revisited? Forests (re)negotiated in the German media between forestry and nature conservation. Forest Policy Econ. 147, 102883. https://doi.org/10.1016/j.forpol.2022.102883.

Mandl, L., Viana-Soto, A., Seidl, R., Stritih, A., Senf, C., 2024. Unmixing-based forest recovery indicators for predicting long-term recovery success. Remote Sens. Environ. 308, 114194. https://doi.org/10.1016/j.rse.2024.114194.

Mermoz, S., Prieto, J.D., Planells, M., Morin, D., Koleck, T., Mouret, F., Bouvet, A., Le Toan, T., Sheeren, D., Hamrouni, Y., Bélouard, T., Paillassa, É., Carme, M., Chartier, M., Martel, S., Féret, J.-B., 2024. Submonthly Assessment of Temperate forest clear-cuts in mainland France. IEEE J. Sel. Top. Appl. Earth Obs. Remote Sens. 17, 13743–13764. https://doi.org/10.1109/JSTARS.2024.3429012.

Olofsson, P., Foody, G.M., Herold, M., Stehman, S.V., Woodcock, C.E., Wulder, M.A., 2014. Good practices for estimating area and assessing accuracy of land change. Remote Sens. Environ. 148, 42–57. https://doi.org/10.1016/j.rse.2014.02.015.

Patacca, M., Lindner, M., Lucas-Borja, M.E., Cordonnier, T., Fidej, G., Gardiner, B., Hauf, Y., Jasinevičius, G., Labonne, S., Linkevičius, E., Mahnken, M., Milanovic, S., Nabuurs, G., Nagel, T.A., Nikinmaa, L., Panyatov, M., Bercak, R., Seidl, R., Ostrogović Sever, M.Z., Socha, J., Thom, D., Vuletic, D., Zudin, S., Schelhaas, M., 2023. Significant increase in natural disturbance impacts on European forests since 1950. Glob. Chang. Biol. 29, 1359–1376. https://doi.org/10.1111/gcb.16531.

Potterf, M., Frühbrodt, T., Thom, D., Lemme, H., Hahn, A., Seidl, R., 2025. Hotter drought increases population levels and accelerates phenology of the European spruce bark beetle Ips typographus. For. Ecol. Manage. 585, 122615. https://doi.org/10.1016/j.foreco.2025.122615.

Rakovec, O., Samaniego, L., Hari, V., Markonis, Y., Moravec, V., Thober, S., Hanel, M., Kumar, R., 2022. The 2018–2020 multi-year drought Sets a new benchmark in Europe. Earth's Future 10, e2021EF002394. https://doi.org/10.1029/2021EF002394.

Reinosch, E., Backa, J., Adler, P., Deutscher, J., Eisnecker, P., Hoffmann, K., Langner, N., Puhm, M., Rüetschi, M., Straub, C., Waser, L.T., Wiesehahn, J., Oehmichen, K., 2024. Detailed validation of large-scale Sentinel-2-based forest disturbance maps across Germany. Forestry Int. J. Forest Res. cpae038. https://doi.org/10.1093/forestry/cpae038.

Schiefer, F., Schmidtlein, S., Frick, A., Frey, J., Klinke, R., Zielewska-Büttner, K., Junttila, S., Uhl, A., Kattenborn, T., 2023. UAV-based reference data for the prediction of fractional cover of standing deadwood from Sentinel time series. ISPRS Open J. Photogram. Remote Sens. 8, 100034. https://doi.org/10.1016/j.ophoto.2023.100034.

Schiefer, F., Schmidtlein, S., Hartmann, H., Schnabel, F., Kattenborn, T., 2024. Large-scale remote sensing reveals that tree mortality in Germany appears to be greater than previously expected. Forestry Int. J. Forest Res. cpae062. https://doi.org/10.1093/forestry/cpae062.

Schiller, C., Költzow, J., Schwarz, S., Schiefer, F., Fassnacht, F.E., 2024. Forest disturbance detection in Central Europe using transformers and Sentinel-2 time

series. Remote Sens. Environ. 315, 114475. https://doi.org/10.1016/j.rse.2024.114475.

Schuldt, B., Buras, A., Arend, M., Vitasse, Y., Beierkuhnlein, C., Damm, A., Gharun, M., Grams, T.E.E., Hauck, M., Hajek, P., Hartmann, H., Hiltbrunner, E., Hoch, G., Holloway-Phillips, M., Körner, C., Larysch, E., Lübbe, T., Nelson, D.B., Rammig, A., Rigling, A., Rose, L., Ruehr, N.K., Schumann, K., Weiser, F., Werner, C., Wohlgemuth, T., Zang, C.S., Kahmen, A., 2020. A first assessment of the impact of the extreme 2018 summer drought on central European forests. Basic Appl. Ecol. 45, 86–103. https://doi.org/10.1016/j.baae.2020.04.003.

Seidl, R., Potterf, M., Müller, J., Turner, M.G., Rammer, W., 2024. Patterns of early post-disturbance reorganization in central European forests. Proc. R. Soc. B 291, 20240625. https://doi.org/10.1098/rspb.2024.0625.

Senf, C., Seidl, R., 2021. Persistent impacts of the 2018 drought on forest disturbance regimes in Europe. Biogeosciences 18, 5223–5230. https://doi.org/10.5194/bg-18-5223-2021.

Shrestha, S.N., Thonfeld, F., Dietz, A., Kuenzer, C., 2025. Prediction of canopy cover loss in german spruce forests using a spatio-temporal approach. Remote Sens. (Basel) 17, 1907. https://doi.org/10.3390/rs17111907.

Spathelf, P., Ammer, C., Annighöfer, P., Bolte, A., Seifert, T., Weimar, H., 2022. Fakten zum Thema: Wälder und Holznutzung. AFZ Der Wald 7, 39–44.

Thonfeld, F., Gessner, U., Holzwarth, S., Kriese, J., da Ponte, E., Huth, J., Kuenzer, C., 2022. A FIRST assessment of canopy cover loss in Germany's forests after the 2018–2020 drought years. Remote Sens. (Basel) 14, 562. https://doi.org/10.3390/rs14030562.

Turubanova, S., Potapov, P., Hansen, M.C., Li, X., Tyukavina, A., Pickens, A.H., Hernandez-Serna, A., Arranz, A.P., Guerra-Hernandez, J., Senf, C., Häme, T., Valbuena, R., Eklundh, L., Brovkina, O., Navrátilová, B., Novotný, J., Harris, N., Stolle, F., 2023. Tree canopy extent and height change in Europe, 2001–2021, quantified using Landsat data archive. Remote Sens. Environ. 298, 113797. https://doi.org/10.1016/j.rse.2023.113797.

Viana-Soto, A., Senf, C., 2025. The European Forest Disturbance Atlas: a forest disturbance monitoring system using the Landsat archive. Earth Syst. Sci. Data 17, 2373–2404. https://doi.org/10.5194/essd-17-2373-2025.

Wang, Y., Rammig, A., Blickensdörfer, L., Wang, Y., Zhu, X.X., Buras, A., 2025. Species-specific responses of canopy greenness to the extreme droughts of 2018 and 2022 for four abundant tree species in Germany. Sci. Total Environ. 958, 177938. https://doi.org/10.1016/j.scitotenv.2024.177938.

Wegler, M., Kacic, P., Thonfeld, F., Holzwarth, S., Jaggy, N., Gessner, U., Kuenzer, C., 2025. Tree species from space: a new product for Germany based on Sentinel-1 and -2 time series. Int. J. Remote Sens. 1–34. https://doi.org/10.1080/01431161.2025.2530236.

Welle, T., Aschenbrenner, L., Kuonath, K., Kirmaier, S., Franke, J., 2022. Mapping dominant tree species of german forests. Remote Sens. (Basel) 14, 3330. https://doi.org/10.3390/rs14143330.

White, J.C., Wulder, M.A., Hermosilla, T., Coops, N.C., Hobart, G.W., 2017. A nationwide annual characterization of 25 years of forest disturbance and recovery for Canada using Landsat time series. Remote Sens. Environ. 194, 303–321. https://doi.org/10.1016/j.rse.2017.03.035.

Winter, C., Müller, S., Kattenborn, T., Stahl, K., Szillat, K., Weiler, M., Schnabel, F., 2025. Forest dieback in drinking water protection areas – a hidden threat to water quality. Earth's Future 13, e2025EF006078. https://doi.org/10.1029/2025EF006078.

Xu, C., Förster, M., Beckschäfer, P., Talkner, U., Klinck, C., Kleinschmit, B., 2025. Modeling European beech defoliation at a regional scale gradient in Germany from northern lowlands to central uplands using geo-ecological parameters, Sentinel-2 and National Forest Condition Survey data. For. Ecol. Manage. 576, 122383. https://doi.org/10.1016/j.foreco.2024.122383.

Zhu, Z., Woodcock, C.E., 2014. Continuous change detection and classification of land cover using all available Landsat data. Remote Sens. Environ. 144, 152–171. https://doi.org/10.1016/j.rse.2014.01.011.